Friction Modeling and Control in Boundary Lubrication *

Pierre E. Dupont and Eric P. Dunlap

Aerospace and Mechanical Engineering
Boston University, Boston, MA 02215

Abstract

It has been known for many years that stick-slip can often be eliminated from a system by stiffening it. More recently, it has been shown that for a negatively-sloped friction-velocity curve, a frictional lag must be present for machine stiffness to produce this stabilizing effect [2,10]. In this paper, experiments involving dry and lubricated line contacts of hardened tool steel are described and a state variable friction model possessing this lag is fit to the data. The model and associated parameter values provide a means for computing lower bounds on the PD gains necessary for steady motion in the boundary lubrication regime.

1   Introduction

It is well known that the discontinuous static-kinetic model is a simple approximation of friction behavior. In actuality, as long as the direction of motion is not reversed, the steady-state friction force is a continuous function of velocity. The slope of this curve depends on the composition of the materials and on the lubricant between them. In general, the friction-velocity curves for hard materials separated by liquid lubricants have steep negative slopes near zero velocity.

The typical shape of the steady-state friction-velocity curve for lubricated contact appears in Figure 1(a). In the region labeled A, corresponding to boundary and mixed lubrication, the curve has a steep negative slope. From a controls viewpoint, a negatively-sloped friction curve is undesirable because it is destabilizing. A small decrease in velocity causes an increase in the retarding friction force which further reduces velocity. A small increase in velocity causes a decrease in the friction force further increasing the velocity. If this curve alone defined friction behavior then stability in region A could only be achieved through high-gain velocity feedback.

This curve, however, describes only steady-state friction. Beginning with Sampson et al. [12] and Rabinowicz [9], it was noted that friction is not determined by current velocity alone; it also depends on the history of motion. This functional relationship for the friction, f, can be
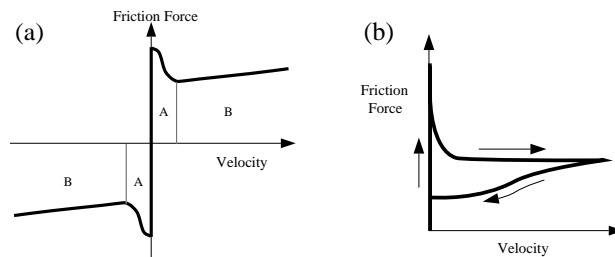
Figure 1: Friction force versus velocity. (a) Steady-state behavior for hard, lubricated surfaces. (b) Multi-branched friction-velocity curve obtained from stick-slip experiments.

expressed as

$$f(t) = \mathcal{F}[V(\tau), \sigma_n(\tau)], \ -\infty < \tau \leq t$$

in which V denotes velocity and σ_n, normal stress. Assuming constant normal stress, this equation describes the evolution of friction between points on the steady-state friction-velocity curve. Since the transient behavior seems to depend on small characteristic sliding distances, its effect is negligible at high velocities, but of critical importance when low velocities are considered.

Dynamic friction models appearing in the literature are most often obtained from stick-slip experiments [1,3,4,7]. The results of these experiments are multi-branched friction-velocity curves similar to Figure 1(b). These experiments all demonstrate that dynamic friction lags the steady-state value.

For the purpose of friction modeling, however, it is desirable to perform experiments in which slip histories are imposed at the friction interface. Hess and Soom [6] is an example of this approach. Furthermore, since friction processes differ between lubrication regimes, it can be equally desirable to develop dynamic friction models based on experiments conducted entirely within one regime. In all papers cited above, however, velocity oscillations overlap several lubrication regimes. For instance, in [6] the mixed, elastohydrodynamic and hydrodynamic lubrication regimes are spanned during each velocity cycle.

Perhaps the most important regime to model is boundary lubrication since high fidelity position and force con-

trol often require achieving stability within this regime. Applications could include high-precision machining and assembly as well as pointing and tracking mechanisms.

In boundary lubrication, the relative velocity between the sliding surfaces is insufficient to develop a separating lubricant film thickness between the surface asperities. Metal to metal contact results producing high friction coefficients and wear in the absence of special boundary lubricants.

In this paper, the results of friction experiments involving dry and lubricated line contacts are presented. The dynamic friction behavior is modeled using a simple state variable friction law. In section 2, state variable friction laws are introduced. The experimental procedure is presented in section 3. Section 4 describes friction for both steady state sliding and velocity steps. The paper concludes with remarks on PD gains for stable sliding.

2 State Variable Friction Models

Research in dynamic friction modeling of rocks in boundary lubrication has been conducted by geophysicists interested in earthquake prediction [5,8,11]. Their models are referred to as state variable friction models. For constant normal stress, the general form, including n state variables, θ_i, is given by

$$f = f(V, \theta_1, \theta_2, \ldots, \theta_n) \tag{1}$$
$$\dot{\theta}_i = g_i(V, \theta_1, \theta_2, \ldots, \theta_n), \quad i = 1, 2, \ldots, n \tag{2}$$

This form implies that a sudden change in velocity cannot produce a sudden change in the state, θ, but does affect its time derivative. For a single state variable, Ruina proposed the following friction law [11].

$$f = f_0 + A \ln(V/V_0) + \theta \tag{3}$$
$$\dot{\theta} = -\frac{V}{L}[\theta + B \ln(V/V_0)] \tag{4}$$

in which θ is the scalar state variable and L is the characteristic sliding length controlling the evolution of θ. The pair (V_0, f_0) corresponds to any convenient point on the steady-state friction-velocity curve. In this case, the steady-state curve is given by

$$f_{ss}(V) = f_0 + (A - B) \ln(V/V_0) \tag{5}$$

and the state variable can be related to the mean lifetime of an asperity junction [8].

If the parameters A and B are such that $A < B$, the steady-state friction-velocity curve is negatively sloped suggesting instability. Rice and Ruina have investigated the system in which a spring, with its free end moving at velocity V_0, pulls a block of mass m across a horizontal frictional surface [10]. They have shown that, for small perturbations, the block velocity will be asymptotically stable at V_0 if the spring stiffness exceeds a critical value, k_{cr}. Generalizing their result to include PD control, k_{cr} is given by

$$k_{cr} = \frac{B - (A + k_v V_0)}{L} \left[1 + \frac{m V_0^2}{(A + k_v V_0) L} \right] \tag{6}$$
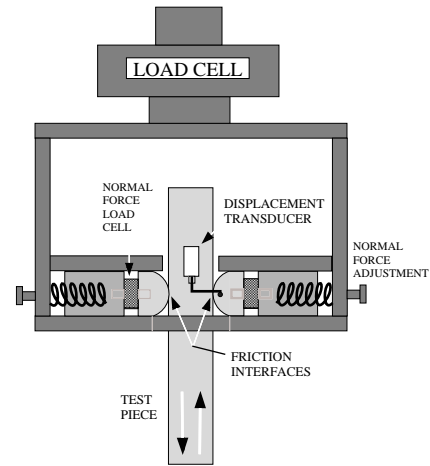

Figure 2: Double-Shear friction fixture. The upper load cell is clamped to a rigid frame while the test piece is clamped to a hydraulic actuator.

where k_v is the derivative control gain. In this case, the combined machine and controller stiffness must exceed k_{cr} for stability.

3 Experiment Design

A servohydraulic materials testing machine was used with the fixture depicted in Figure 2 for the friction experiments. The fixture applies normal stresses through the two semi-cylindrical riders to the flat test piece. The double-shear design, while averaging the friction at the two interfaces, doubles the friction force sensitivity. As pictured, soft springs are used to maintain a relatively constant normal stress. Load cells, in series with each rider, are used to detect any changes in normal force during a trajectory. The load cell at the top of the fixture measures friction force.

Displacement of the friction interfaces is measured by a linear variable differential transformer (LVDT). This transducer is mounted on the unstressed portion of the test piece adjacent to the interfaces. Its output is used by a digital PID controller for interface motion control. The controller is attached to a PC through which interface trajectories are programmed. The PC also records data from the position and force sensors during the tests. Since displacement is measured very close to the friction interfaces, the measurement does not include most elastic deformation of the fixture and test pieces. The maximum allowable displacement of the actuator, 2 mm, corresponds to that of the LVDT.

4 Experimental Results

Friction behavior was investigated for both steady sliding and step changes in velocity in the range of 0.1 to 200 μm/sec. Three lubrication conditions were studied: dry, paraffin oil with maximum Saybolt viscosity of 158 and a

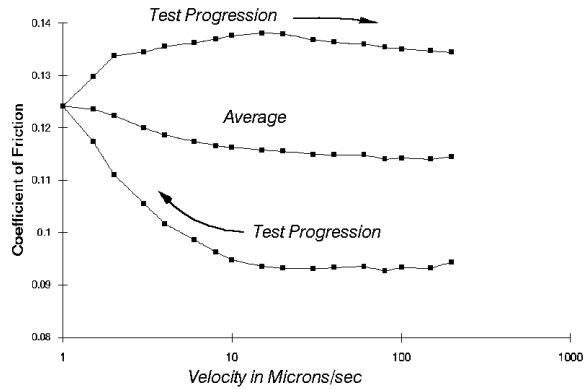Figure 3: Effect of lubricant depletion and wear on steady state friction for boundary lubricant. Order of velocity passes is shown.

Figure 4: Collecting average steady state friction data by applying multiple velocity steps during a single pass.

commercial boundary lubricant paste. All samples were made of A.I.S.I. Grade 1 tool steel which was heat treated and oil quenched to a surface Rockwell hardness of 59C.

All tests were conducted with a normal force of 100 N. This value was chosen to avoid excessive wear while also considering the sensitivity of the friction force load cell. The maximum change in normal force observed during any trial was 5%. To minimize contamination, separate test and interface pieces were used for the different lubricants. Between each trial, the pieces were lightly polished with 600 grit paper, washed with acetone and lubricated. After lubrication, the surfaces were run in by pulling, then pushing, the test piece through its maximum displacement, 2 mm, at 20 μm/sec.

4.1 Steady State Sliding

A steady-state friction versus velocity curve (or Stribeck curve) is usually assembled from a collection of points, where each point corresponds to the average friction recorded during a constant-velocity trial. Initially, friction-velocity curves were compiled by averaging constant-velocity data for 2 mm tensile displacements run sequentially (without relubrication) at fifteen velocities. The sequence began with the highest velocity, proceeded to the lowest, and then continued until the highest velocity was reached again. As seen in Figure 3 for the boundary lubricant, friction changed appreciably between the first trials and the last. In these instances, the long-term memory of sliding history can be just as important as the short-term memory embodied in the state variable model.

To minimize the effect of accumulated sliding during the progression of steady-state tests, an alternate scheme for producing friction-velocity curves was adopted. In this scheme, velocity steps were made every 250 μm of displacement. The test sequence began with the lowest velocity, reached a maximum midway along the test piece, and then decreased, finishing with the initial minimum velocity. Figure 4 depicts a portion of one trial for paraf-
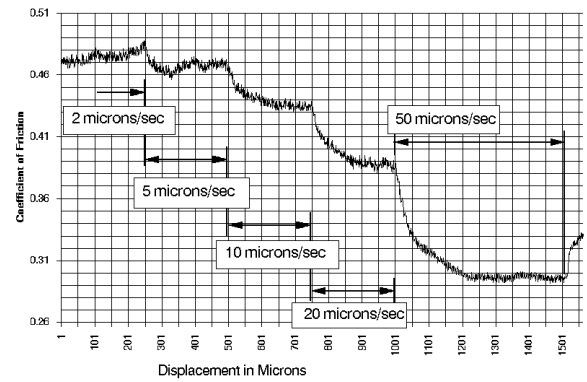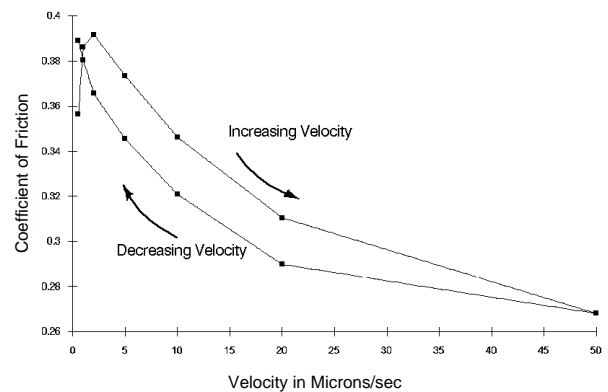

Figure 5: Steady state friction for paraffin oil based on eight trials using the method of Figure 4.

fin oil. The average friction force for each velocity was computed using the data from the last 50 μm of displacement at that velocity. In this way, data for seven velocities could be collected twice in a single pass during which the displacement history of the test piece is essentially constant. While the riders (interface pieces) do experience wear during each trial, the effect of this wear appeared to be minimal.

The average of eight trials conducted this way for paraffin oil are shown in Figure 5. For each trial, as well as the average depicted, friction following step increases in velocity exceeded that following step decreases in velocity. (An exception was the initial and final velocity of 0.5 μm/sec.) This effect was observed in our data even when the order of velocities was reversed. This behavior is similar to the loops reported by Hess and Soom in response to an oscillating velocity of constant sign [6]. The loops suggest that steady state was not achieved after 200 μm of sliding. However, with a standard deviation of ±20%, error bars about the points in Figure 5 would enclose the loop. For this reason, it was decided that stepping through fewer velocities per trial would be of no additional value.
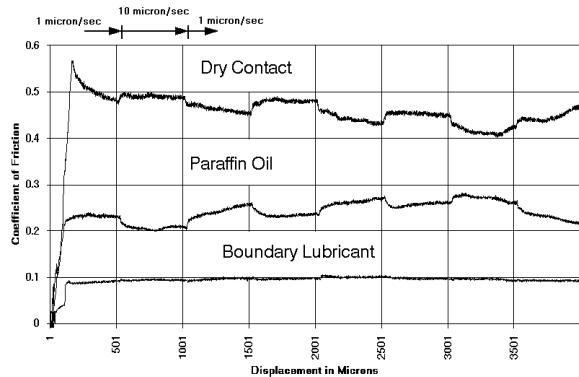
Figure 6: Comparison of lubrication conditions during alternating velocity steps occurring 500 μm apart.

4.2 Dynamic Friction Behavior

The evolution of friction force between points on the steady-state friction-velocity curve was studied by imposing step changes in velocity at the friction interface. The hydraulic actuator produced velocity steps with a rise time of less than 0.5 seconds corresponding to a displacement of less than 5 μm for the velocities considered.

The three lubrication conditions are compared in Figure 6 for velocity steps alternating between 1 and 10 μm/sec. The effectiveness of the boundary lubricant can be seen from its low friction coefficient and its minimal response to velocity steps (at this scale). In addition, the steady state friction coefficients of the poor lubricants, dry and paraffin oil, drift considerably and exhibit more "noise". The boundary lubricant and paraffin oil usually exhibited a negative dependence of friction on velocity. In dry contact, a negative dependence was often observed for new samples which evolved to a positive dependence after repeated trials without relubrication. A positive dependence is depicted in Figure 6. While this effect is stabilizing, the associated high friction and wear rate are undesirable.

The response of the state variable friction law described by (3) and (4) to a velocity step imposed at time t_0 is shown in Figure 7. Let the pair (V_1, f_1) correspond to the initial steady state, (V_2, f_2) describe the steady state reached after the velocity jump and $f_{\max}$ be the maximum friction force during the transient. The parameters A and B, normalized by constant normal force N, can be computed from test data using

$$A_\mu = A/N = \frac{f_{\max} - f_1}{N \ln(V_2/V_1)} \qquad (7)$$

$$B_\mu = B/N = A_\mu - \frac{f_2 - f_1}{N \ln(V_2/V_1)} \qquad (8)$$

The exponential decay of the state variable θ following a velocity step is described by

$$\theta = B(e^{-V_2 t/L} - 1) \ln(V_2/V_1) \qquad (9)$$

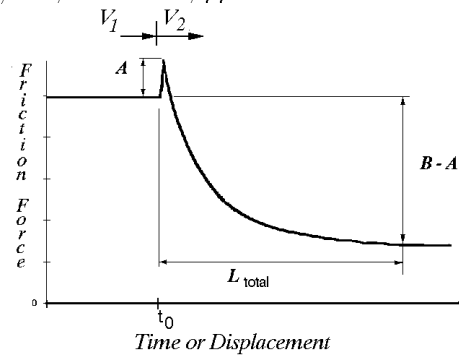The characteristic sliding length, L, was computed from

Figure 7: State variable model parameters from step response.

a least squares fit of the exponential to the data immediately following the velocity step. Determination of B and L was complicated in some cases by the variation in steady state friction after the step. Three curve fits were made for each jump using values of f_2 computed as averages of 200-point data windows starting 50, 100 and 250 μm after the step. These windows are depicted in Figure 8. The best fit of the three was selected as the one with the largest coefficient of determination. The parameter values obtained in this way were averaged over at least eight trials for each lubricant. The means and standard deviations of the means appear in Table 1.

The instantaneous response to velocity changes, measured by parameter A, was observed in many of the dry and boundary lubricant tests. A single boundary lubricant trial clearly depicts this effect in Figure 9. For paraffin oil, this effect, if present, was less than the noise level of the load cell. This can be observed from Figure 4.

Considering the relative magnitude of inertial forces, perturbations about steady sliding are often essentially quasistatic. When this condition is met, the expression for critical stiffness reduces to (assuming $k_v = 0$)

$$k_{cr} = \frac{(B_\mu - A_\mu)N}{L} \qquad (10)$$

The critical stiffnesses of the three lubrication conditions appear in Table 1. They represent a lower bound on the combined machine and controller stiffness for asymptotic stability of the linearized system.

5 Discussion and Conclusions

For the tested material and lubricants, the velocity step response of friction can be modeled quite well with the single state variable friction law of Ruina. To the authors' knowledge, the existence of an instantaneous viscosity, modeled by A, has not been previously reported for lubricated engineering materials.

Using the state variable model, it was possible to compute a lower bound on system stiffness for steady sliding. What is perhaps surprising is that the unlubricated system has the smallest critical stiffness. This is due primarily to a
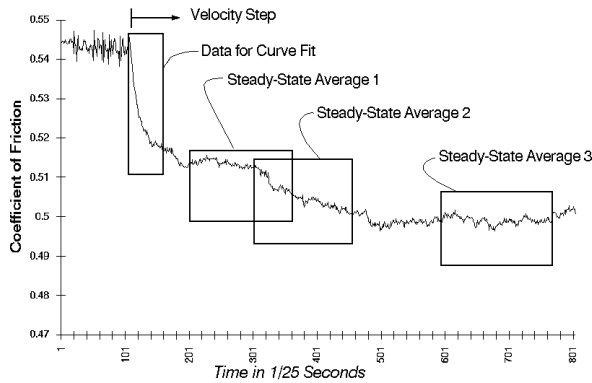
Figure 8: Curve fitting of exponential decay to typical friction data.

Parameter	Dry	Paraffin Oil	Boundary Lubricant
$A_\mu \times 10^3$	2.8 ± 0.5	0.0^*	1.1 ± 0.1
$B_\mu \times 10^3$	9.4 ± 1.1	11.1 ± 2.5	4.0 ± 0.4
L (μm)	64.7 ± 14.3	22.4 ± 4.3	19.2 ± 1.4
k_{cr} (kN/m)	10.2 ± 2.9	49.4 ± 14.5	14.8 ± 2.3

Table 1: State variable model parameter values for velocity jumps in the range 1 - 10 μm/sec. * The magnitude was less than the noise level of the load cell.

characteristic sliding length, L, three times as large as that of the lubricated cases. As noted earlier, with continued sliding, the dry surfaces often exhibited a positive dependence of friction on velocity. In these situations, k_{cr} reduces to zero.

Paraffin oil inhibited any instantaneous dependence of friction on velocity and produced a large negative steady-state dependence. While the latter effect may lead to low friction coefficients at higher velocities, it necessitates a large system stiffness for stability in the boundary lubrication regime.
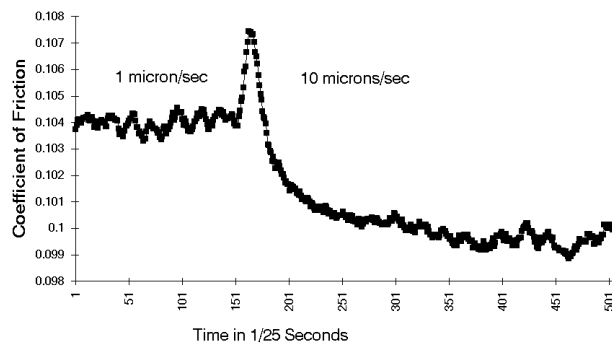

Figure 9: Single trial showing step response of boundary lubricant.

As expected, the boundary lubricant produced a low steady-state friction coefficient and also provided good transient performance. While its characteristic sliding length is close to that of paraffin oil, it produces significant instantaneous damping as well as a small negative steady-state friction-velocity slope. Its critical stiffness is less than a third of that of paraffin oil.

The parameters and critical stiffnesses reported in Table 1 provide useful benchmarks for predicting system stability as well as for further research. While beyond the scope of this paper, $\ln(V)$ did not linearize steady-state friction over the entire range of 0.1 to 200 μm/sec as predicted by (5). More work is needed in this area.

6   References

1. S. Antoniou, A. Cameron and C. Gentle, "The Friction-Speed Relation from Stick-Slip Data." *Wear*, Vol. 36, pp. 235-54, 1976.

2. B. Armstrong-Hélouvry, **Control of Machines with Friction**, Kluwer Academic Press, 1991.

3. R. Bell and M. Burdekin, "A Study of the Stick-slip Motion of Machine Tool Feed Drives." *Proc. Institute Mechanical Engineers*, Vol. 184, Pt. 1, No. 29, pp. 543-60, 1969.

4. L. Bo and D. Pavelescu, "The Friction-Speed Relation and its Influence on the Critical Velocity of Stick-Slip Motion." *Wear*, Vol. 82, No. 3, pp. 277-89, 1982.

5. J.H. Dieterich, "Micro-mechanics of Slip Instabilities with Rate- and State-dependent Friction." (Abstract), Fall Meeting Abstract Volume, Eos, Trans. Am. Geophys. Union, pp. 324, 1991.

6. D. Hess and A. Soom, "Friction at a Lubricated Line Contact Operating at Oscillating Sliding Velocities." *ASME J. Tribology*, Vol. 112, No. 1, pp. 147-52, January 1990.

7. S. Kato and T. Matsubayashi, "On the Dynamic Behavior of Machine-tool Slideway – 1st Report, 2nd Report." *Bull. Jap. Soc. Mech. Eng.*, Vol. 13, No. 55, pp. 170-88, 1970.

8. M. Linker and J. Dieterich, "Effects of Variable Normal Stress on Rock Friction: Observations and Constitutive Equations." *J. of Geophysical Research*, Vol. 97, No. B4, pp. 4923-40, 1992.

9. E. Rabinowicz, "A Study of the Stick-Slip Process." *Friction and Wear*, Ed. Robert Davies, Elsevier Publishing Co., New York, 1959.

10. J. Rice and A. Ruina, "Stability of Steady Frictional Slipping." *J. of Applied Mechanics*, Vol. 50, No. 2, pp. 343-49, June 1983.

11. A. Ruina, "Friction Laws and Instabilities: A Quasistatic Analysis of Some Dry Frictional Behavior." Ph.D. Dissertation, Division of Engineering, Brown University, 1980.

12. J. Sampson, F. Morgan, D. Reed and M. Muskat, "Friction Behavior During the Slip Portion of the Stick-Slip Process." *J. of Applied Physics*, Vol. 14, No. 12, pp. 689-700, December 1943.